Supporting information of

Multi-contrast magnetic resonance imaging of visual white matter pathways in patients with glaucoma

Authors: Shumpei Ogawa[1)*], Hiromasa Takemura[2,3,4,5)*], Hiroshi Horiguchi[1)], Atsushi Miyazaki[6)], Kenji Matsumoto[7)], Yoichiro Masuda[1)], Keiji Yoshikawa[1,8)], Tadashi Nakano[1)]

Affiliations:

1. Department of Ophthalmology, The Jikei University School of Medicine, Tokyo, Japan
2. Center for Information and Neural Networks (CiNet), Advanced ICT Research Institute, National Institute of Information and Communications Technology, Suita, Japan
3. Graduate School of Frontier Biosciences, Osaka University, Suita, Japan
4. Division of Sensory and Cognitive Brain Mapping, Department of System Neuroscience, National Institute for Physiological Sciences, Okazaki, Japan
5. Department of Physiological Sciences, School of Life Science, SOKENDAI (The Graduate University for Advanced Studies), Hayama, Japan
6. Global Education Center, Waseda University, Tokyo, Japan.
7. Brain Science Institute, Tamagawa University, Machida, Japan
8. Yoshikawa Eye Clinic, Machida, Japan

* These authors contributed equally

Supplementary Materials and Methods

Defining the Lateral Geniculate Nucleus (LGN) region of interest (ROI) for tractography

In this study, we did not acquire high-resolution proton density (PD)-weighted images for visualizing the LGN [1,2] because the acquisition of high-resolution PD-weighted images requires a longer acquisition time, which is difficult to apply for patient experiments. Nevertheless, an accurate definition of the LGN at the single voxel level is not necessary for the purpose of this study, as the goal is to define the approximate position of the LGN for tractography, rather than a detailed analysis of the LGN per se.

Instead of directly visualizing the LGN, we used the method described in a previous study [3]. In brief, we first performed deterministic tractography using the optic chiasm as seed voxels. We then inspected T1-weighted images to determine the location of the endpoints of the streamlines from the optic chiasm. We then defined the LGN ROI by placing a 4-mm radius sphere covering the endpoints of the streamlines. The size of the ROI is sufficiently large to cover the LGN of healthy and glaucomatous subjects [4], and comparable to the LGN volume reported in previous works [5,6]. Moreover, a previous study [3] demonstrated that the location of the LGN identified by this method is consistent with that in histological data [7]. Therefore, the precision of the LGN ROI defined in this study is sufficiently accurate for tractography of the optic tract (OT) and optic radiation (OR).

Tract identification: OT

We used ConTrack [8], which is a part of the vistasoft software (https://github.com/vistalab/vistasoft), to identify OT from the dMRI data. We generated 5,000 candidate streamlines connecting the optic chiasm identified by FreeSurfer [9] and the LGN ROI identified by the above procedure (angle threshold, 90°; step size, 1 mm; maximum streamline length, 80 mm) in both hemispheres. Tracking was performed separately for the two runs of the dMRI data. The OT streamlines were refined by the subsequent steps of outlier removal. We first excluded biologically implausible OT streamlines that pass through the white matter inferior to the hippocampus, corpus callosum or fornix by manually drawing exclusion ROIs in these regions. We then

removed streamlines passing through voxels where the mean diffusivity exceeded 1 μm^2/msec to exclude streamlines interfacing with the cortico-spinal fluid (CSF). In addition, using the Automatic Fiber Quantification (AFQ) MATLAB toolbox (https://github.com/yeatmanlab/AFQ) [10], we excluded streamlines that met the following criteria: (1) streamline length ≥ 3 S.D. longer than the median streamline length in the tract, (2) streamline position ≥ 3 S.D. away from the median position of the tract. Finally, we further removed streamlines whose median distance to the tract core among all the nodes was larger than the distance threshold (1.5 mm) [3].

Tract identification: OR

The OR was also identified using ConTrack [8], which is a dedicated software to identify the OR from the dMRI data [11]. We generated 100,000 candidate streamlines connecting the LGN and V1 ROIs identified using the Brodmann atlas in FreeSurfer (angle threshold, 90°; step size, 1 mm; maximum streamline length, 240 mm). We refined the OR streamlines by following the outlier rejection steps. Tracking was performed separately for the two runs of the dMRI data. First, we selected 30,000 streamlines with the highest scores in the ConTrack scoring process [8]. Second, we removed streamlines passing through voxels where the mean diffusivity exceeded 1 μm^2/msec to exclude streamlines interfacing with lateral ventricles. Third, we excluded biologically implausible OR streamlines traversing the white matter inferior to the hippocampus or passing through the corpus callosum using manually drawn exclusion ROIs. Finally, we further excluded streamlines that met the following criteria: (1) streamline length ≥ 4 S.D. longer than the median streamline length in the tract, (2) streamline position ≥ 4 S.D. away from the median position of the tract, using the AFQ MATLAB toolbox [10].

Supplementary Figures

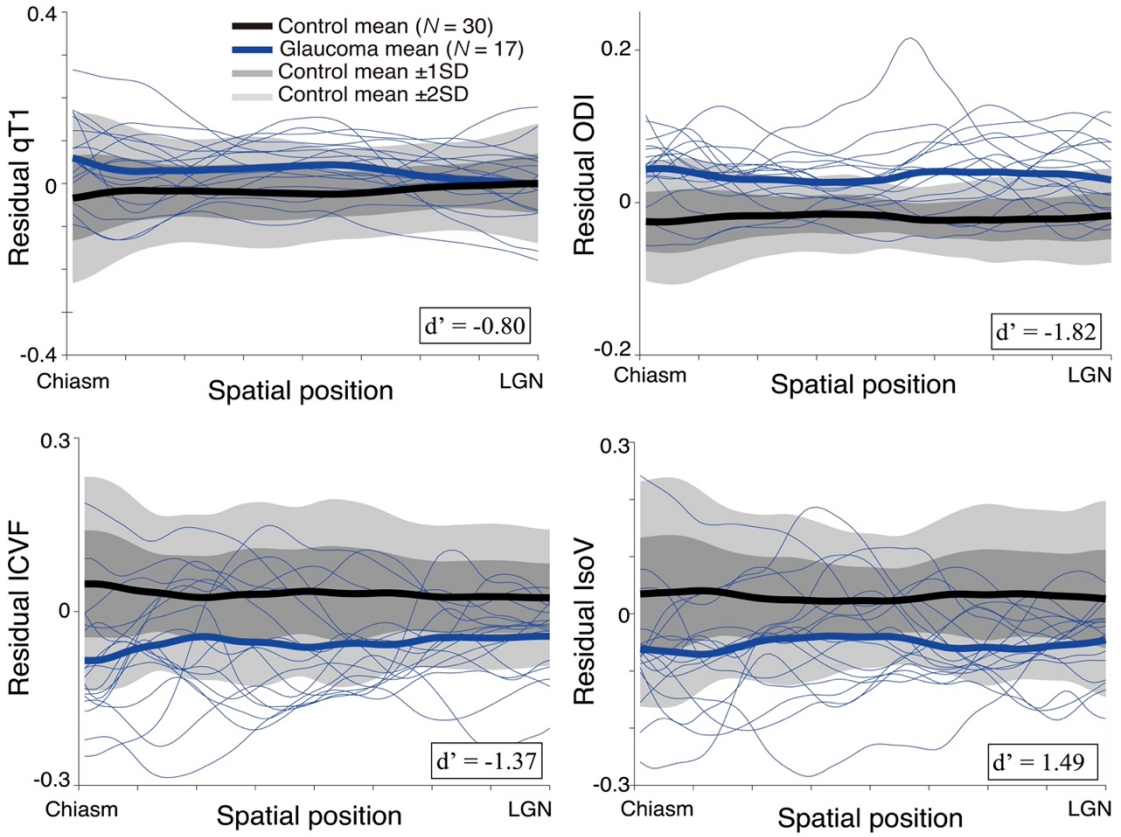

Supplementary Figure 1. Tissue properties along the OT after using linear regression to control for inter-subject variability in age (see Materials and Methods). The vertical axis depicts the residual of each metric (qT1, ICVF, ODI, and IsoV), which describes the inter-subject variance not explained by age variability. Other conventions are identical to those in Figure 3.

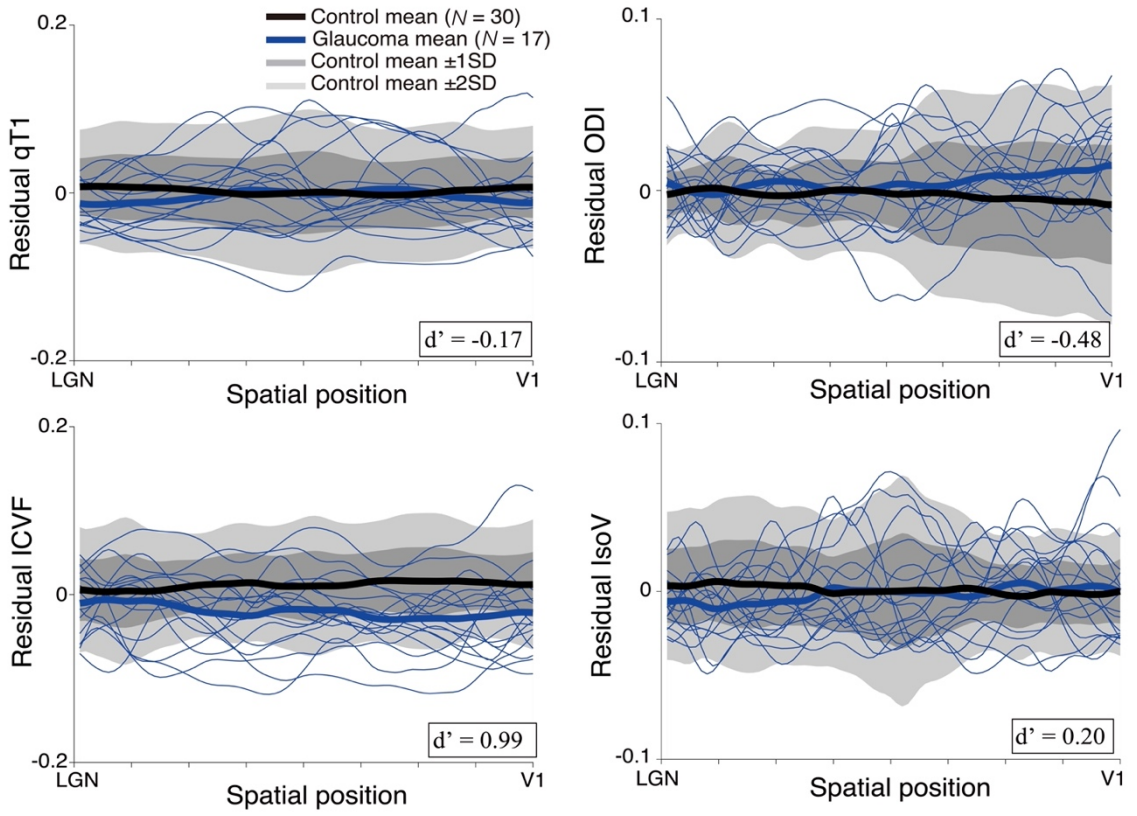

Supplementary Figure 2. Tissue properties along the OR after using linear regression to control for inter-subject variability in age (see Materials and Methods). Other conventions are identical to those in Supplementary Figure 1.

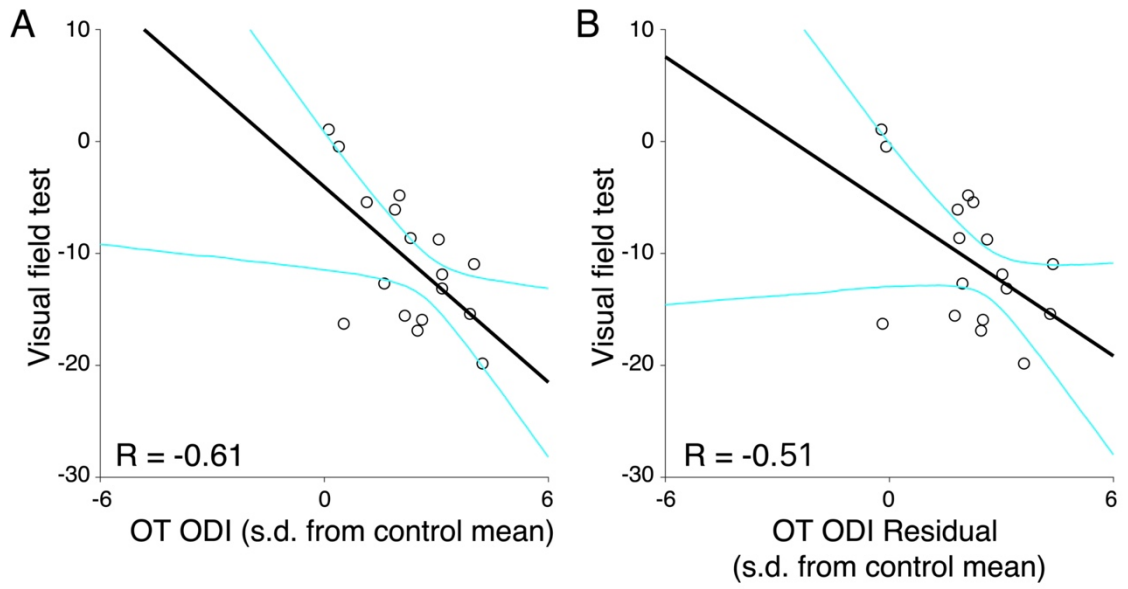

Supplementary Figure 3. Comparison of MRI measurements and results of the visual field test. A. Correlation between white matter tissue properties (ODI along the OT) and the visual field test results in patients with glaucoma. **B.** Correlation between white matter tissue properties controlled for patient age (ODI along the OT) and the visual field test results.

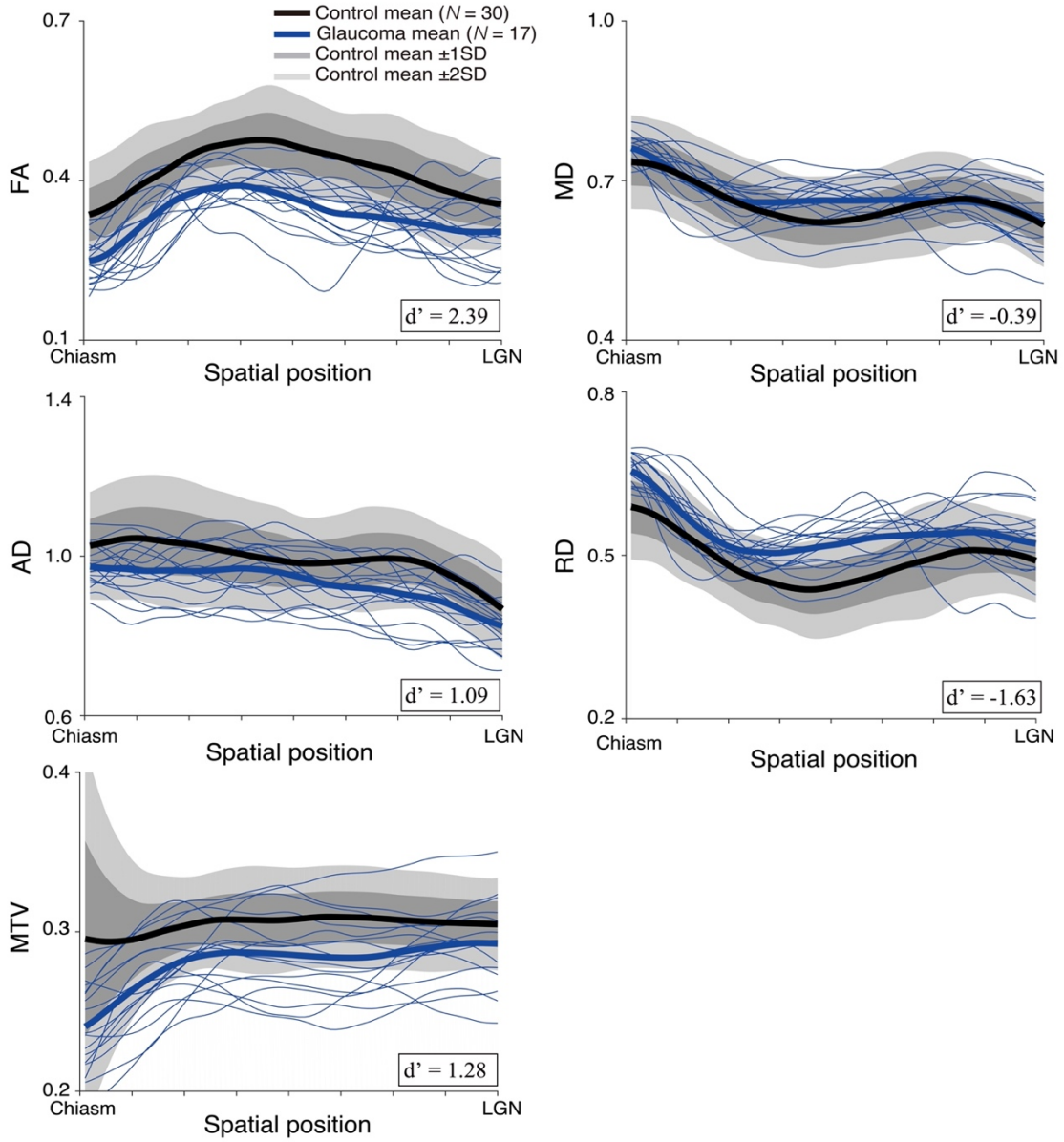

Supplementary Figure 4. Tissue properties along the OT evaluated by other types of MRI-based metrics (FA, MD, AD, RD, and MTV). Conventions are identical to those in Figure 3.

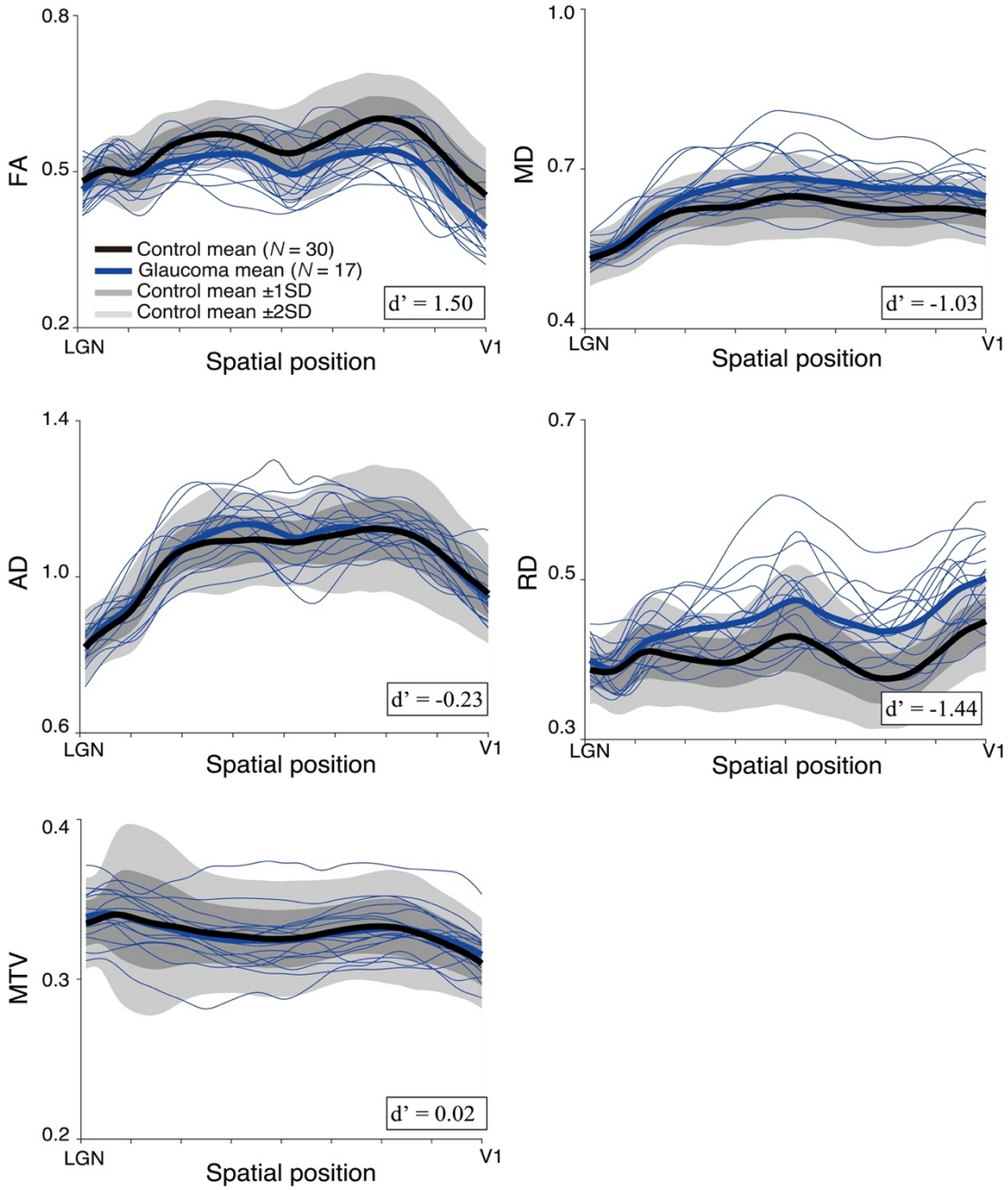

Supplementary Figure 5. Tissue properties along the OR evaluated by other types of MRI-based metrics (FA, MD, AD, RD, and MTV). Conventions are identical to those in Figure 4.

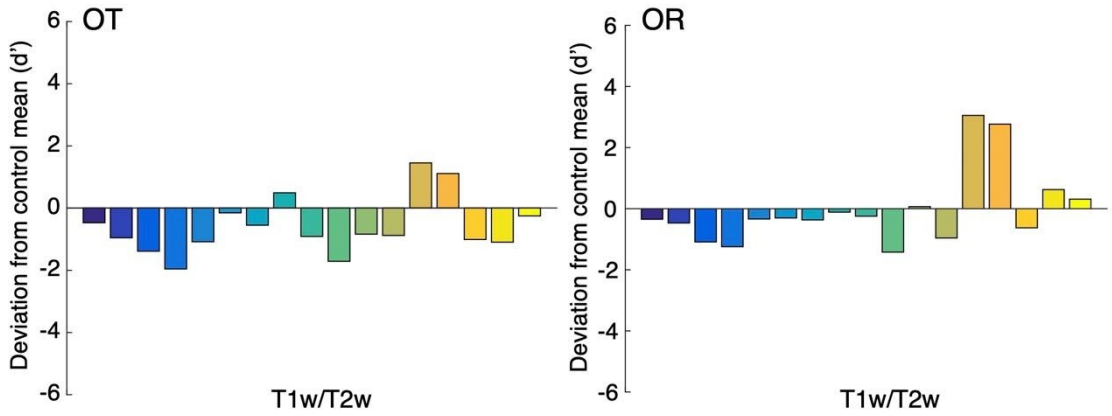

Supplementary Figure 6. T1w/T2w ratio measurements in patients with glaucoma. *Left panel*: OT. *Right panel*: OR. The vertical axis of each plot represents the extent to which individual patients with glaucoma (color bars; Glc001-017) deviated from the control mean (*N* = 25). Conventions are identical to those used in Figure 6.

Supplementary Table 1. Correlations between metrics along the OT in healthy controls.

	ICVF	ODI	IsoV
qT1	R = 0.10	R = 0.33	R = 0.15
ICVF		R = 0.30	R = 0.43
ODI			R = -0.07

Supplementary Table 2. Correlations between metrics along the OR in healthy controls.

	ICVF	ODI	IsoV
qT1	R = -0.56	R = -0.27	R = 0.16
ICVF		R = 0.48	R = -0.11
ODI			R = -0.29

Supplementary Table 3. Correlations between metrics along the OT in patients with glaucoma.

	FA	MD	RD	AD
ICVF	R = 0.52	R = -0.64	R = -0.86	R = -0.20
ODI	R = -0.90	R = -0.46	R = -0.10	R = -0.88
IsoV	R = 0.70	R = 0.05	R = -0.45	R = 0.37

Supplementary Table 4. Correlations between metrics along the OR in patients with glaucoma.

	FA	MD	RD	AD
ICVF	R = 0.53	R = -0.95	R = -0.88	R = -0.77
ODI	R = -0.53	R = -0.43	R = -0.03	R = -0.85
IsoV	R = -0.30	R = 0.38	R = 0.40	R = 0.24

References

1. Viviano JD, Schneider KA. Interhemispheric interactions of the human thalamic reticular nucleus. *J Neurosci*. 2015;35(5):2026-2032.

2. Oishi H, Takemura H, Amano K. Macromolecular tissue volume mapping of lateral geniculate nucleus subdivisions in living human brains. *bioRxiv*. Published online 2020. https://www.biorxiv.org/content/10.1101/2020.12.26.424373v1.abstract

3. Takemura H, Ogawa S, Mezer AA, et al. Diffusivity and quantitative T1 profile of human visual white matter tracts after retinal ganglion cell damage. *Neuroimage Clin*. 2019;23:101826.

4. Gupta N, Greenberg G, de Tilly LN, Gray B, Polemidiotis M, Yücel YH. Atrophy of the lateral geniculate nucleus in human glaucoma detected by magnetic resonance imaging. *Br J Ophthalmol*. 2009;93(1):56-60.

5. DeSimone K, Viviano JD, Schneider KA. Population Receptive Field Estimation Reveals New Retinotopic Maps in Human Subcortex. *J Neurosci*. 2015;35(27):9836-9847.

6. Kastner S, O'Connor DH, Fukui MM, Fehd HM, Herwig U, Pinsk MA. Functional imaging of the human lateral geniculate nucleus and pulvinar. *J Neurophysiol*. 2004;91(1):438-448.

7. Amunts K, Lepage C, Borgeat L, et al. BigBrain: an ultrahigh-resolution 3D human brain model. *Science*. 2013;340(6139):1472-1475.

8. Sherbondy AJ, Dougherty RF, Ben-Shachar M, Napel S, Wandell BA. ConTrack: finding the most likely pathways between brain regions using diffusion tractography. *J Vis*. 2008;8(9):15.1-16.

9. Fischl B. FreeSurfer. *Neuroimage*. 2012;62:774-781.

10. Yeatman JD, Dougherty RF, Myall NJ, Wandell BA, Feldman HM. Tract profiles of white matter properties: automating fiber-tract quantification. *PLoS One*. 2012;7:e49790.

11. Sherbondy AJ, Dougherty RF, Napel S, Wandell BA. Identifying the human optic radiation using diffusion imaging and fiber tractography. *J Vis*. 2008;8(10):12.1-11.